



# An algorithm for coalescence of classical objects and formation of planetary systems

Søren Toxvaerd<sup>a</sup>

Department of Science and Environment, Roskilde University, Postbox 260, DK-4000 Roskilde, Denmark

Received: 19 November 2021 / Accepted: 24 December 2021

© The Author(s), under exclusive licence to Società Italiana di Fisica and Springer-Verlag GmbH Germany, part of Springer Nature 2022

**Abstract** Isaac Newton formulated the central difference algorithm (Eur. Phys. J. Plus (2020) 135:267) when he derived his second law. The algorithm is under various names (“Verlet, leap-frog,..”) the most used algorithm in simulations of complex system in Physics and Chemistry, and it is also applied in Astrophysics. His discrete dynamics has the same qualities as his exact analytic dynamics for continuous space and time with time reversibility, symplecticity and conservation of momentum, angular momentum and energy. Here, the algorithm is extended to include the fusion of objects at collisions. The extended algorithm is used to obtain the self-assembly of celestial objects at the emergence of planetary systems. The emergence of twelve planetary systems is obtained. The systems are stable over very long times, even when two “planets” collide or if a planet is engulfed by its sun.

## 1 Introduction

Simulations of collections of classical objects in the Universe have been performed for many decades [1–8]. The coupled second-order differential equations have either been solved numerically by various higher-order symplectic algorithms [3, 9–12] or by the particle–particle/particle–mess (PPPM) method [13]. In the PPPM method, each mass unit, e.g., a planet is treated as moving in the collective field of all others, and the Poisson equation for the PPPM grid is solved numerically. Later, simulations with large-scaled computer packages [14, 15] with many billions of mass units show strong evidence for dark matter in the Universe. A comprehensive review of the simulations, the mass distribution in the Universe and the evidence for dark matter is given in [16].

The present algorithm and the simulations deviate from the previous algorithms and the PPPM model and the complex simulations in several ways. The basic algorithm is the central difference algorithm. It appears in the literature under different names, most known as the “Verlet-” or “leap-frog” algorithm, but it is actually first formulated by Isaac Newton in PHILOSOPHIÆ NATURALIS PRINCIPIA MATHEMATICA in 1687 [17, 18]. In celestial mechanics, it has been rediscovered as the second-order leap-frog discrete mapping [3, 9, 10] and extended to higher order [11, 12]. Newtons discrete expression for the relation between the positions of the objects, their forces and the discrete time propagation is time reversible, symplectic and has the same dynamic invariances for a conservative system as his analytic formulation [19, 20]. The algorithm allows for obtaining the discrete dynamics of classical objects without any approximations, and here his algorithm is extended to cover the fusions of objects and self-assembly at the emergence of planetary systems.

## 2 The discrete algorithm for fusion of classical objects

According to Newton’s classical discrete dynamics, a new position  $\mathbf{r}_k(t + \delta t)$  at time  $t + \delta t$  of an object  $k$  with the mass  $m_k$  is determined by the force  $\mathbf{f}_k(t)$  acting on the object at the discrete position  $\mathbf{r}_k(t)$  at time  $t$  and the position  $\mathbf{r}_k(t - \delta t)$  at  $t - \delta t$  as

$$m_k \frac{\mathbf{r}_k(t + \delta t) - \mathbf{r}_k(t)}{\delta t} = m_k \frac{\mathbf{r}_k(t) - \mathbf{r}_k(t - \delta t)}{\delta t} + \delta t \mathbf{f}_k(t). \quad (1)$$

where the momenta  $\mathbf{p}_k(t + \delta t/2) = m_k(\mathbf{r}_k(t + \delta t) - \mathbf{r}_k(t))/\delta t$  and  $\mathbf{p}_k(t - \delta t/2) = m_k(\mathbf{r}_k(t) - \mathbf{r}_k(t - \delta t))/\delta t$  are constant in the time intervals in between the discrete positions. Newton *postulated* Eq. (1) and obtained his second law from Eq. (1) as the limit  $\lim_{\delta t \rightarrow 0}$  [18].

Newton is together with Leibniz the fathers of analytic mathematics and Newton’s discrete algorithm- or equivalent expressions, is usually presented as a third-order predictor algorithm, which can be derived by a Taylor–McLaurin expansion from the objects analytic trajectories. Brook Taylor (1685–1731) lived at the same time as Newton (1643–1727), and Newton had full knowledge of Taylor expansions, but Newton never presented his expression for his second law, even in his later two editions of *Principia*,

<sup>a</sup> e-mail: [st@ruc.dk](mailto:st@ruc.dk) (corresponding author)

as the first and leading term in an analytic expansion. And with good reason because, unlike algorithms obtained by higher-order expansions, his discrete algorithm has all the qualities of the analytic analog.

Isaac Newton obtained his second law as the limit expression  $\lim_{\delta t \rightarrow 0}$  of the central difference in momentum for a planet at a discrete change  $\delta t$  in time. But he noticed in *Principia* at the derivation of the law that the areas of three triangles in his geometrical construction of the discrete trajectory of a planet are equal, an irrelevant observation for the derivation, but he did not mention the consequence of the equal areas. It is Kepler’s second law, and the young Newton must immediately, when he postulated the law have realized, that his discrete relation Eq. (1) at least explains Kepler’s second law. But he did not mention it at the derivation of the second law, even much later when he wrote *Principia*, nor in his second- or third editions of *Principia* [17]. The fulfillment of Kepler’s second law is a consequence of the conserved angular momentum in his discrete dynamics [22]. An explanation for that Newton on the one hand noticed the equality of the areas of the triangles, and on the other hand did not notice that this explains Kepler’s second law could be, that he believed that the exact classical dynamics first is achieved in the analytic limit with continuous time and space. But this is in fact not the case, his discrete dynamics has the same invariances as his analytic dynamics. Due to the time symmetry, it is time reversible and the algorithm is also symplectic [3,9,10,23]. The conservation of momentum and angular momentum is ensured by Newton’s second and third law, because the sum of the forces between the objects in a conservative system is zero. The algorithm conserves also the energy, but it is, however, not obvious because of the asynchronous appearance of positions and momenta, and thereby the asynchronous determination of the potential- and the kinetic energy. But one can prove that the discrete algorithm conserves the energy [20] and also show that there (most likely) exists a ”shadow Hamiltonian” nearby the Hamiltonian for the analytic dynamics and where the discrete positions are located on the shadow Hamiltonian’s analytic trajectories [19,21,22]. So the discrete dynamics has a constant energy given by the energy of the shadow Hamiltonian. Newton’s discrete algorithm has been rediscovered several times, most known by L. Verlet [24], and it appears with a variety of names: Verlet-, Leap-frog,...[22]. Almost all molecular dynamics (MD) simulations of complex physical and chemical systems and many celestial mechanics simulations are performed with Newton’s discrete algorithm.

It is convenient to reformulate Newton’s algorithm as the “Leap frog” algorithm

$$\mathbf{v}_k(t + \delta t/2) = \mathbf{v}_k(t - \delta t/2) + \delta t/m_k \mathbf{f}_k(t), \tag{2}$$

with the velocities  $\mathbf{v}(t + \delta t/2)$  and  $\mathbf{v}(t - \delta t/2)$  and the positions

$$\mathbf{r}_k(t + \delta t) = \mathbf{r}_k(t) + \delta t \mathbf{v}_k(t + \delta t/2), \tag{3}$$

so the new positions at  $t + \delta t$  are obtained in two steps, first by calculating the new (mean) velocities  $\mathbf{v}_k(t + \delta t/2)$  in the time interval  $[t, t + \delta t]$  from the old velocities  $\mathbf{v}_k(t - \delta t/2)$  in the previous time interval and the forces  $\mathbf{f}_k(\mathbf{r}_k(t))$  at the positions  $\mathbf{r}_k(t)$ , and then the new positions  $\mathbf{r}_k(t + \delta t)$  are obtained from the velocities  $\mathbf{v}_k(t + \delta t/2)$ .

Newton’s discrete algorithm is here used as a starting point for a formulation of a discrete algorithm for the irreversible fusion of spherical symmetrical objects by classical dynamics with inelastic collisions. The derivation of the algorithm is governed by a desire to preserve as much as possible of the invariances of Newton’s dynamics.

### 2.1 An algorithm for coalescence of classical objects and formation of planetary systems

The classical discrete dynamics between  $N$  spherically symmetrical objects with masses  $m^N = m_1, m_2, \dots, m_N$  and positions  $\mathbf{r}^N(t) = \mathbf{r}_1, \mathbf{r}_2, \dots, \mathbf{r}_N$  is obtained by Eq. (2) and Eq.(3) with extensions.

According to Newton’s shell theorem [25], the force,  $\mathbf{F}_i$ , on a spherically symmetrical object  $i$  with mass  $m_i$  is a sum over the forces,  $\mathbf{f}(r_{ij})$ , caused by the other spherically symmetrical objects  $j$  with mass  $m_j$ , and it is solely given by their center of mass distance  $r_{ij}$  to  $i$

$$\mathbf{F}_i(r_{ij}) = \sum_{j \neq i}^N \mathbf{f}(r_{ij}) = -\frac{Gm_i m_j}{r_{ij}^2} \hat{\mathbf{r}}_{ij}. \tag{4}$$

Let all the spherically symmetrical objects have the same (reduced) number density  $\rho = (\pi/6)^{-1}$  by which the diameter  $\sigma_i$  of the spherical object  $i$  is

$$\sigma_i = m_i^{1/3} \tag{5}$$

and the collision diameter

$$\sigma_{ij} = \frac{\sigma_i + \sigma_j}{2}. \tag{6}$$

If the distance  $r_{ij}(t)$  at time  $t$  between two objects is less than  $\sigma_{ij}$  the two objects merge to one spherical symmetrical object with mass

$$m_\alpha = m_i + m_j, \tag{7}$$

and diameter

$$\sigma_\alpha = (m_\alpha)^{1/3}, \tag{8}$$

and with the new object  $\alpha$  at the position

$$\mathbf{r}_\alpha = \frac{m_i}{m_\alpha} \mathbf{r}_i + \frac{m_j}{m_\alpha} \mathbf{r}_j, \tag{9}$$

at the center of mass of the two objects before the fusion. (The object  $\alpha$  at the center of mass of the two merged objects  $i$  and  $j$  might occasionally be near another object  $k$  by which more objects merge, but after the same laws.)

Let the center of mass of the system of the  $N$  objects be at the origin, i.e.,

$$\sum_k m_k \mathbf{r}_k(t) = \mathbf{0}. \tag{10}$$

The momenta of the objects in the discrete dynamics just before the fusion are  $\mathbf{p}^N(t - \delta t/2)$  and the total momentum of the system is conserved at the fusion if

$$\mathbf{v}_\alpha(t - \delta t/2) = \frac{m_i}{m_\alpha} \mathbf{v}_i(t - \delta t/2) + \frac{m_j}{m_\alpha} \mathbf{v}_j(t - \delta t/2), \tag{11}$$

which determines the velocity  $\mathbf{v}_\alpha(t - \delta t/2)$  of the merged object.

The invariances in the classical Newtonian dynamics are for a conservative system with Newton’s third law, i.e., with

$$\mathbf{f}_{kl}(t) = -\mathbf{f}_{lk}(t) \tag{12}$$

for the forces between two objects  $k$  and  $l$ , and with no external forces. An object  $k$ ’s forces with  $i$  and  $j$  before the fusion are  $\mathbf{f}_{ik}(t)$  and  $\mathbf{f}_{jk}(t)$ , and these forces must be replaced by calculating the force  $\mathbf{f}_{\alpha k}(\mathbf{r}_{\alpha k}(t))$ . The total force after the fusion is zero due to Newtons third law for a conservative system with the forces  $\mathbf{f}_{\alpha k} = -\mathbf{f}_{k\alpha}$  between pairs of objects, and the total momentum

$$\begin{aligned} \sum_k \mathbf{p}_k(t_n + \delta t/2) &= \sum_k \mathbf{p}_k(t_n - \delta t/2) + \delta t \sum_k \mathbf{f}_k(t_n) \\ &= \sum_k \mathbf{p}_k(t_n - \delta t/2), \end{aligned} \tag{13}$$

and the position of the center of mass are conserved for the discrete dynamics with fusion.

The determination of the position,  $\mathbf{r}_\alpha(t)$  and the velocity,  $\mathbf{v}_\alpha(t - \delta t/2)$ , of the new object from the requirement of conserved center of mass and conserved momentum determines the discrete dynamics of the  $N - 1$  objects.

The angular momentum is affected by the fusion. The angular momentum of the system of spherically symmetrical objects consist of two terms

$$\mathbf{L}(t) = \mathbf{L}_G(t) + \mathbf{L}_I(t) \tag{14}$$

where  $\mathbf{L}_G(t)$  is the angular momentum of the objects due to the dynamics obtained from the gravitational forces between their center of masses, and  $\mathbf{L}_I(t)$  is the angular momentum due to the spin of the objects. Without fusion  $\mathbf{L}_G(t)$  is conserved for Newtons discrete dynamics [22].  $\mathbf{L}_I(t)$  is, however, also conserved according to the shell theorem [25], where Newton proves that no net gravitational force is exerted by a shell on any object inside, regardless of the object’s location within the uniform shell, by which the spin of the object is not affected by any force and is therefore constant. But at a fusion  $\mathbf{L}_G$  changes by

$$\delta \mathbf{L}_G(t) = \mathbf{r}_\alpha(t) \times m_\alpha \mathbf{v}_\alpha(t - \delta t/2) - \mathbf{r}_i(t) \times m_i \mathbf{v}_i(t - \delta t/2) - \mathbf{r}_j(t) \times m_j \mathbf{v}_j(t - \delta t/2). \tag{15}$$

and  $\mathbf{L}_I$  changes by

$$\begin{aligned} \delta \mathbf{L}_I(t) &= (\mathbf{r}_i(t) - \mathbf{r}_\alpha(t)) \times m_i \mathbf{v}_i(t - \delta t/2) + (\mathbf{r}_j(t) - \mathbf{r}_\alpha(t)) \times m_j \mathbf{v}_j(t - \delta t/2) \\ &= \mathbf{r}_i(t) \times m_i \mathbf{v}_i(t - \delta t/2) + \mathbf{r}_j(t) \times m_j \mathbf{v}_j(t - \delta t/2) - \mathbf{r}_\alpha(t) \times m_\alpha \mathbf{v}_\alpha(t - \delta t/2) \\ &= -\delta \mathbf{L}_G(t). \end{aligned} \tag{16}$$

So without fusion the angular momenta  $\mathbf{L}_I(t)$  and  $\mathbf{L}_G(t)$  with Newton’s discrete dynamics are conserved separately, and at a fusion the total angular momentum is still conserved but with an exchange of angular momentum with  $\delta \mathbf{L}_I(t) = -\delta \mathbf{L}_G(t)$ .

The exact classical discrete dynamics with fusion of colliding objects can be used to explore the self-assembly at the emergence of planetary systems and to investigate the stability and chaotic behavior of solar systems [26].

### 3 Simulation of formation of planetary systems

The algorithm Eqs.(2), (3) and IIA is used to simulate the emergence of planetary systems. The setup of the actual MD systems and the general conditions for MD for gravitational systems is given in the Appendix. Our planetary system is presumably created from flattened, rotationally supported disc structures of cosmic dust grains, and the composition of the building blocks–planetesimals—is grossly different from that of the sun [27]. Here, the results for twelve MD simulations of the emergence of planetary systems are presented. The planetary systems are obtained from different diluted “gas” states of  $N = 1000$  objects with equal masses and

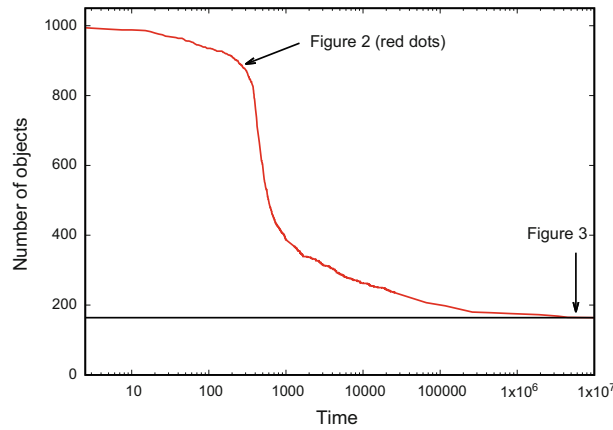


**Fig. 1** The number  $N(t)$  of objects (sun, planets and free objects) as a function of time  $t$  with fusion for one (No. 1) of the twelve systems. This system contained 852 objects at  $t = 250$ . The positions of the  $N=852$  objects are shown in Fig. 2 (red dots) together with the start positions with  $N = 1000$  (small blue dots). At  $t = 4.5 \times 10^6$  the planetary system contained one Sun and 165 planets and free objects, and the system aged with only one fusion for the succeeding  $\Delta t = 5.5 \times 10^6$  time. The planet orbits at  $t = 4.5 \times 10^6$  for four inner planets are shown in Fig. 3

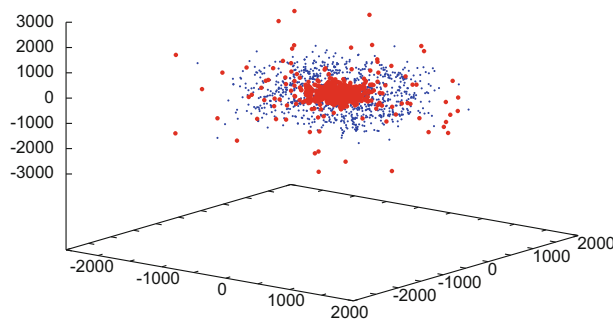


**Fig. 2** The positions of the  $N$  objects at the start of fusion with small blue dots, and with red dots at  $t = 250$  where the fusion accelerated (Fig. 1) and ended with one sun, 23 planets and 142 free objects

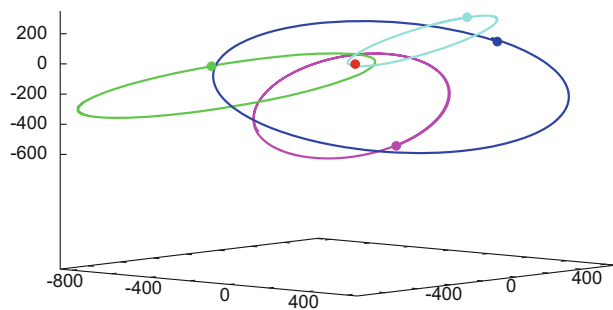


**Fig. 3** The sun (red, enlarged) with four planets close to the sun. The orbits are obtained at  $t = 4.50 \times 10^6$  after creation of the solar system. Light blue: Orbit time  $T_{\text{orbit}} = 630$ , eccentricity  $\epsilon = 0.941$ ; green:  $T_{\text{orbit}} = 1308$ ,  $\epsilon = 0.867$ ; blue  $T_{\text{orbit}} = 1740$ ,  $\epsilon = 0.377$ ; magenta  $T_{\text{orbit}} = 1529$ ,  $\epsilon = 0.815$ . The light blue planet has circulated  $\approx$  seven thousand times around the sun

at different low temperatures (mean velocity of the objects), and the systems can be considered as embryos of planetary systems by self-assembly of simple small grains.

The creation of a system with one heavy central object and with some of the other objects in orbits around the central “sun” is established within a relative short period of time as illustrated in Fig. 1. The start configurations are diluted spherical (gas) distributions of objects (see Appendix). The objects are accelerated toward the center of mass by the gravitational forces, and the fusion of objects results in a creation of a system with one heavy object (the sun) and with other of the objects in elliptical orbits around the sun. The solar systems are created rather quickly. The system No. 1 (Figs. 1, 2, 3, 4, 5 and Table 1) is established already after a fusion time  $t \approx 1000$  (see Fig. 1, for MD details and unit of time see Appendix) with 386 objects consisting of one sun with the mass  $m_{\text{sun}} = 557$  and many planets and free objects. Nine of the planets have a mass  $m = 3$ , but most of the other planets and free objects (338) are not fused with others and have a mass  $m = 1$ . The solar system is in a rather stable state but ages slowly (Fig. 1). First after  $t = 4.5 \times 10^6$  are all twelve planetary system stable and with very rare mergers (Table I). The four planets in

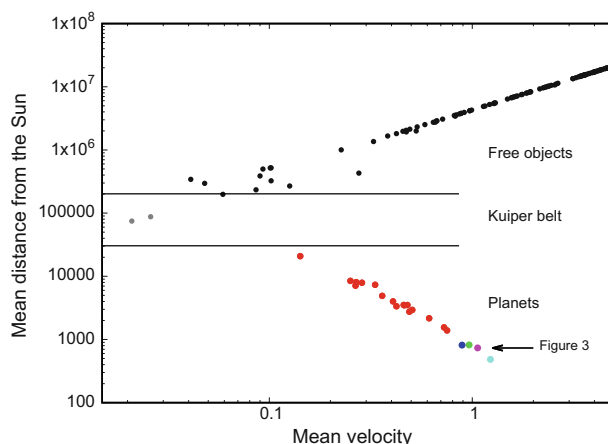
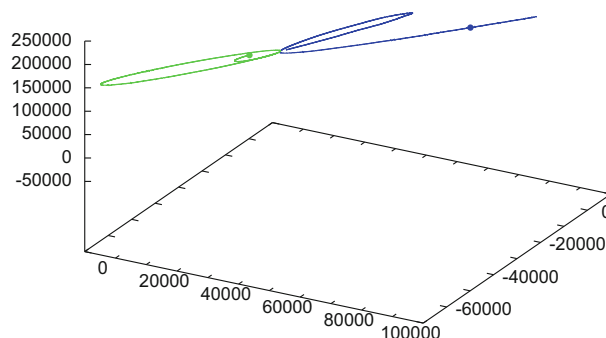


**Fig. 4** Mean  $\log$ –distances ( $\log \langle r_{i,\text{sun}}(t) \rangle$ ) to the sun of the objects  $i$  as a function of their relative ( $\log$ ) mean velocities  $\log \langle v_{i,\text{sun}}(t) \rangle$  for planetary system No. 1. The means are for a time interval  $\Delta t \in [4.0 \times 10^6, 4.5 \times 10^6]$ . The locations of the four inner planets in Fig. 3 are marked with their color from Fig. 3. The planets (colored spheres) are located on the lower branch of the distribution and the upper branch shows (black spheres) the mean locations of the free objects. The “Kuiper belt” with these objects (grey spheres) is estimated to be for mean locations  $\approx \langle r_{i,\text{sun}}(t) \rangle \in [30000, 200000]$ . Orbits of planets in the Kuiper belt are shown in the next Fig.

**Fig. 5** Two planets in the “Kuiper belt.” The planet shown with green changed its course, but remained in the Kuiper belt, whereas the planet shown with blue escaped the planetary system



planetary system No. 1 closest to the sun are shown in Fig. 4. The angular momentum,  $\mathbf{L}_G$ , of the planetary system is constant if there is no fusion, but also the angular momenta of the individual planets are also almost constant. The four planets shown in Fig. 4 have almost constant angular momenta with closed elliptical orbits.

The solar system shown in Figs. 1, 2, 3, 4 is system No. 1 (see Table 1). It consists of many planets including very tiny bounded planets in a “Kuiper belt” and with orbits which have an orbit time of more than  $t_{\text{orbit}} = 1 \times 10^5$ . The existence of such Kuiper belt makes it difficult to determine precisely how many planets a planetary system consists of since the planets change their orbits over time. The distribution of planets and free objects is determined from the distances and velocities relative to the sun. A planet will have a relative short mean distance to the sun, averaged over a long time interval, whereas a free object has a long mean distance and a constant velocity. Figure 4 shows the relative mean distances of the objects to the sun as a function of their relative mean velocities, where the means are obtained for  $\Delta t \in [4.0 \times 10^6, 4.5 \times 10^6]$ . The distribution has two branches, a lower branch for the planets and an upper branch for the free objects.

The Kuiper belt is located in between the two branches in Fig. 4. The objects in this zone are almost free from the gravitational attractions of the sun and the other planets, and sometimes an object in this zone escapes from the planetary system. Figure 5 shows two planets in the Kuiper belt, where one (green) remained in the planetary system, whereas one (blue) escaped. The planet with green remained in the planetary system and with elliptical-like orbits. The planet with green was in an elliptical orbit with an eccentricity

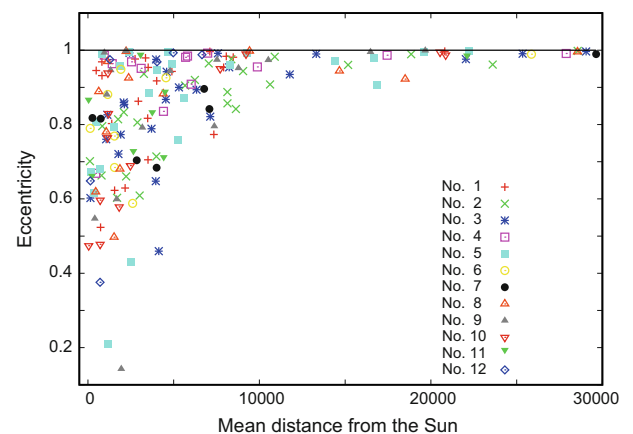
$$\epsilon = \frac{r_{\text{max}} - r_{\text{min}}}{r_{\text{max}} + r_{\text{min}}} = \frac{156090 - 115}{156090 + 115} = 0.9985, \tag{17}$$

and with the longest distance  $r_{\text{max}} = 156090$  at aphelion and the shortest distance at perihelion  $r_{\text{min}} = 115$ . The orbit time is  $5.06 \times 10^5$ . After passing the aphelion at  $r_{i,\text{sun}}=156090$ , the planet ended in a new elliptical orbit closer to the sun with a new aphelion distance  $r_{i,\text{sun}}=38635$ . The other object shown with blue in Fig. 5 escaped the planetary system.

Our Solar system has a Kuiper belt located  $\approx 30$ – $100$  AU (astronomical unit = mean distance between the Earth and the Sun). This distance is translated to the present solar systems by setting  $1 \text{ AU}=500$ , i.e.,  $\approx$  equal to the mean distance of one of the inner planets in Fig. 4 (light blue). The lower border of the present Kuiper belt should be  $\approx 30 \times 500 = 15000$  with this unit and the

**Table 1** Collected data for the planetary systems

No.	Inner Planets	"Kuiper planets	Free objects	$m_{\text{Sun}}$	$\langle r_{\text{cl}} \rangle$	Temp.
1	21	2	142	830	484	4.24
2	25	10	317	628	119	8.88
3	24	10	229	720	150	11.60
4	13	5	224	739	455	12.53
5	23	7	253	700	191	10.76
6	8	3	116	865	131	5.00
7	7	0	147	839	262	19.08
8	13	4	182	765	452	3.45
9	15	6	159	779	402	4.62
10	12	2	141	826	44	3.95
11	8	2	107	862	43	4.76
12	6	2	90	897	145	4.65

**Fig. 6** The eccentricity of the planets in the twelve planetary systems as a function of their mean distances from their suns

upper border should be  $\approx 50000$ . The planet orbit shown with green in Fig. 5 has a maximum distance 156090. The present Kuiper belt in planetary system No. 1 is estimated to be in the interval  $|\mathbf{r}(t) - \mathbf{r}_{\text{sun}}(t)| \in [30000, 200000]$ .

The data for the twelve simulations of planets systems are collected in Table I. The data are obtained in the time interval  $t \in [4.0 \times 10^6, 4.50 \times 10^6]$  after the start of the fusions. The mean distances  $\langle r_{\text{cl}} \rangle$  are the mean distance to the sun for the planet in a system closest to the sun. The temperatures,  $T$ , of the objects are obtained from the mean kinetic energy  $\langle E_{\text{Kin}} \rangle / N = 3/2T$ , and the different start distributions and kinetic energies of the objects result in temperatures which varies with a factor of  $\approx 4$ . There is, however, no clear connection between the number of planets and the mean kinetic energies of the planetary systems.

The eccentricities and mean positions of planets in the twelve systems are shown in Fig. 6. The distributions show that the inner planets in general have an eccentricity significant below  $\epsilon = 1$ , which is the limit of stability for an elliptical orbit, whereas the planets close to the border of the Kuiper belt ( $\approx 30000$ ) all have eccentricities only little less than the limit of stability.

#### 4 Conclusion

Newton solved in *Principia* as the first, Kepler's equation and determined the analytic expression for the orbit of a planet -or a comet, but the analytic dynamics of a solar system with many planets can only be obtained numerically, traditionally by the use of higher order symplectic algorithms. But the discrete dynamics with Newtons central difference algorithm is also time reversible and symplectic and has the same invariances as his analytic classical dynamics. Here, his discrete algorithm is extended to handle fusion of objects at a collision and to create small planetary systems.

The formation of a planetary system depends on the distribution and the kinetic energies of the collection of objects that start to fuse together. Our planetary system is presumably created from flattened, rotationally supported disc structures of cosmic dust grains, and the composition of the building blocks—planetesimals—is grossly different from that of the sun [27]. Here, twelve planetary systems are created by fusions of a small number  $N = 1000$  objects (planetesimals) with equal masses and from a spherical starting distribution of the merging objects, in order to test the algorithm and to obtain an "embryo" of a planetary system. The time

evolutions in the systems reveal that the objects spontaneously form “mini” planetary systems with a heavy “sun” and with many of the planetesimals in orbits around the sun. The planetary systems have some qualities which agree with our own Solar system, with stable elliptical orbits and with many bounded objects at great distances from the sun in a “Kuiper belt.” But the planetary systems deviate from the Solar system by, that the orbits are not in a common Ecliptic plane due to the spherically distributed starting positions of the merging objects. Furthermore, there is no planetary systems with moons. These deviations can, however, very well be a consequence of the small size of the systems with only  $N = 1000$  spherically distributed objects at the start of the fusion, and to the monodispersity of the systems with equal masses of the objects at the start. The small systems was selected in order to be able to follow the created solar systems over very long times without any approximations in order to test the exact algorithm and the aging and stability of the planetary systems.

The planetary systems are established over a short period of time with fusions. The systems are stable and age slowly by that a planet occasionally collided with another planet or with the sun and merge. Some of the planets were also accelerated out of the planetary system (Fig. 5). The planetary systems show chaotic sensitivity, and the actual numbers of inner planets and their positions and eccentricities depend on the forces from all the other objects in the system, including the free objects far from the sun. Almost all of the twelve planetary systems contain many planets in Kuiper belts far from the suns.

The extension of Newton’s discrete dynamics with the algorithm for fusion of colliding objects is the simplest possible. The fusion of two spherical symmetrical objects to one uniform and spherical symmetrical object is far from what actually happens when two macroscopic celestial bodies merge [28]. But, although it is straight forward to extend the algorithm to a more complex fusion at the collision, it has not be the goal with the present investigation. The algorithm is suitable for analysis of the self-assembly of planetesimals and, due to the exact dynamics, the algorithm can be useful at investigations of the impact of the chaotic behavior on the stability of planetary systems.

**Acknowledgements** This work was supported by the VILLUM Foundation Matter project, grant No. 16515.

**Data Availability Statement** Data will be available on request.

## 5 Appendix: Molecular dynamics simulation of planetary systems

The simulations of the creation of planetary systems were performed for different numbers  $N = 100, 1000$  and  $10000$  of objects and for different start configurations of the objects. The spherically symmetrical objects are identical and interact with the gravitational force Eq. (4). All units (mass, time, length, energy/force) are given in units given by  $G, m_i$  and  $\sigma_i$ , and the present simulations are started with  $N = 1000$  objects with equal masses  $m_i = 1$  and diameter  $\sigma_i = 1$ . In order to simulate the orbit of a planet near the sun, it is necessary to choose a small time increment  $\delta t = 0.0025$  [22]. The MD simulations are with double-precision variables, the center of mass and the momentum and orbits of planets are conserved after more than  $10^9$  time steps with a small time increment  $\delta t = 0.0025$ .

The phase space diagram for the gravitational system [29] differs from a traditional phase space diagram. A collection of objects will, without fusion collapse at low temperature (velocities of the objects) and relative high concentration in the collection [30], but at high temperatures and low concentrations the collection of objects expands continuously in the space. The collapsed spherical symmetrical objects will, without fusion perform a crystal. It is as mentioned not possible to obtain a traditional phase diagram for a classical system with gravitational forces because the energy per object

$$\begin{aligned} u/kT &= 2\pi\rho \int_0^\infty u(r)g(r)r^2 dr \\ &\approx -2\pi\rho Gm_1m_2 \int_0^\infty r_{12}dr_{12} \end{aligned} \quad (18)$$

(and free energy) diverges for an uniform distribution. The objects crystallize at low temperatures if the objects perform elastic collisions without fusion. In contrast to this behavior, the collections of free objects at low temperatures and concentrations and with fusion merge into solar systems with planets in regular orbits. The algorithm with fusions is used obtain planetary systems.

Here, we shall describe twelve simulations of the emergence of planetary systems for  $N = 1000$  and for diluted gas configurations of the objects at the start, which are spherically (blue dots in Fig. 3). The twelve systems are generated for different start configurations and kinetic energies. The momenta and angular momenta  $\mathbf{L}_G(0)$  at the start  $t = 0$  are adjusted to zero.

Depending on the start configurations of positions and kinetic energy, the systems either collapse at low kinetic energy and high gas density into one heavy object (black hole), or expand in the open space for high kinetic energy and low density. But in between these ranges of velocities and concentrations some objects merge with creation of one heavy object (the sun), with planets and with unbounded objects. (A free object is characterized by the fact that it, with a constant direction with respect to the sun and with a positive energy  $E = E_{\text{Kin}} + E_{\text{Pot}}$ , increases its distance to the sun.)

The twelve systems are started at different mean “temperatures”  $T$  in the interval  $T \in [0.1, 0.5]$ . The fusions started shortly after (Fig. 2) with an increase in the mean velocities. The total momenta and the center of masses and angular momenta  $\mathbf{L}$  are conserved,

but the angular momenta  $\mathbf{L}_G$  are not conserved at the fusions, but varied within the range  $\mathbf{L}_G \approx [-\mathbf{10}, -\mathbf{10}]$ . The random round-off errors in the double precision arithmetic have no effect on the orbits of the planets. The simulations were performed by consecutive simulations with  $2 \times 10^8$  time steps. At the start of a simulation, the center of mass and momentum components were adjusted to zero, and by the end of a simulation the round-off errors had changed the center of mass components from  $\approx 10^{-18}$  to  $\approx 10^{-16}$ . The components of the momentum were changed with the same factor. These tiny adjustments have, however, no effect on the stability, nor on the orbits of the planetary systems.

Without any approximations, the dynamics of a planetary systems is time demanding because one needs a rather small time increment  $\delta t$  to obtain the orbit of a planet at Perihelion accurately, and the stability of the planetary system is given by its long-time behavior, which together implies that it is necessary to performs billions of time steps in order to obtain the long-time behavior of a planetary system. The present calculations are for  $n = 1.8 \times 10^9$  time steps ( $t = 4.5 \times 10^6$ ). Another complication is that the computational time without some approximations varies with the number  $N$  of objects as  $\propto N^2$ . It is, however, straight forward to implement different kind of time consuming approximations used in MD [13, 31] whereby the computational time varies proportional to  $\approx N$ .

## References

1. A.A. Kyyipin, S.F. Shandarin, MNRAS **204**, 891 (1983)
2. J. Centrella, A.L. Melott, Nature **305**, 196 (1983)
3. J. Wisdom, M. Holman, AJ *102*, 1528 (1991)
4. M. J. Duncan, H. F. Levison, M. H. Lee, AJ *116*, 2067 (1998)
5. J.E. Chambers, G.W. Wetherill, Icarus **136**, 304 (1998)
6. J. Laskar, P. Robutel, Celest. Mech. Dyn. Astron. **80**, 39 (2001)
7. H. Rein, D. Tamayo, 2015, MNRAS *452*, 376 (2015)
8. H. Rein, G. Brown, D. Tamayo, MNRAS **490**, 5122 (2019)
9. E. Forest, R.D. Ruth, Physica D **43**, 105 (1990)
10. H. Youshida, Phys. Lett. A **150**, 262 (1990)
11. D.M. Hernandez, E. Bertschinger, MNRAS **452**, 1934 (2015)
12. A.C. Petit, J. Laskar, G. Boué, M. Gastineau, A&A **628**, A32 (2019)
13. R.W. Hockney, S.P. Goel, J.W. Eastwood, J. Comput. Phys. **14**, 148 (1974)
14. J. Diemand et al., Nature **454**, 735 (2008)
15. J.-M. Alimi et al., SC2012: International Conference for High Performance Computing, Networking, Storage and Analysis. IEEE Computer Soc. Press, 2012, CA p. 1
16. I. de Martino et al., Universe **6**, 107 (2020)
17. I. Newton, PHILOSOPHIÆ NATURALIS PRINCIPIA MATHEMATICA. LONDINI, Anno MDCLXXXVII. Second Ed.1713; Third Ed. 1726
18. *Principia*, PROPOSITION 1. THEOREM 1
19. S. Toxvaerd, Phys. Rev. E **50**, 2271 (1994)
20. S. Toxvaerd, J. Chem. Phys. **140**, 044102 (2014)
21. S. Toxvaerd, J.O. Heilmann, J.C. Dyre, J. Chem. Phys. **136**, 224106 (2012)
22. S. Toxvaerd, Eur. J. Phys. **135**, 267 (2020)
23. S. Toxvaerd, Phys Rev. E *47*, 343 (1993)
24. L. Verlet, Phys. Rev. **159**, 98 (1967)
25. *Principia*, THEOREM XXXI
26. D.M. Hernandez, S. Hadden, J. Makino, MNRAS **493**, 1913 (2020)
27. J. Blum, G. Wurm, Annu. Rev. Astron. Astrophys. **46**, 21 (2008)
28. R.M. Canup, E. Asphaug, Nature **412**, 708 (2001)
29. X. Hernandez, Entropy **14**, 848 (2012)
30. B. Lindblad, Nature **125**, 133 (1935)
31. S. Toxvaerd, J.C. Dyre, J. Chem. Phys. **134**, 081102 (2011)